IV.I.25 Integrated Nanoscale Metal Hydride – Catalyst Architectures for Hydrogen Storage

Yiping Zhao[a], Jin Z. Zhang[b]
and Matthew D. McCluskey[c]
[a] Department of Physics and Astronomy,
The University of Georgia
[b] Department of Chemistry and Biochemistry,
University of California – Santa Cruz
[c] Department of Physics and Astronomy,
Washington State University

Contract Number: (DE-FG02-05ER46251)

Progress Report: (May 2008 – Apr. 2009)

1. Fabrication of Mg Nanoblades and Catalyst-Loaded Mg Nanostructures

We have designed and installed a unique GLAD system with two e-beam sources for the fabrication of nanostructured hydrogen storage materials (such as Mg, MgNi alloy, catalyst coated/doped Mg and its alloy, multilayered metal nanostructures). Due to the reactive nature of the metals/metal alloys for hydrogen storage, the system integrates the vacuum chamber with a glove box. This unique system shown in Figure 1 is the first of its kinds in the world.

Using the unique GLAD system, we have fabricated Mg thin film using normal deposition configuration,

FIGURE 1. The unique GLAD system designed for this project.

and Mg nanoblade by GLAD with an incident angle $\alpha \geq 70°$. The as-deposited Mg film shows a typical columnar structure, and its surface consists of piles of nanoflakes, overlapping with one another. The as-deposited GLAD sample shows a well-aligned nanoblade array structure with a blade thickness of tens to hundreds of nm (similar to Figures 1a and b). The thickness of the Mg nanoblades along the incident vapor direction is markedly thinner than the width perpendicular to the incident vapor direction. In addition, by combining the GLAD technique with multilayer deposition and dynamic shadowing growth, one can deposit a thin layer of catalyst to coat the two sides of individual Mg nanoblades, and thus form catalyst decorated Mg nanoblade array structure. With two e-beam sources, a technique called glancing angle co-deposition (GLACD) can be used to fabricate catalyst-doped Mg nanostructures. The GLACD technique is a combination of co-deposition and GLAD. The co-deposition provides a way to evaporate two or more materials simultaneously to form composite or doped material, while the GLAD technique provides a way to form aligned nanorod arrays and to design the topological shape of the nanostructures. The composition of the resulting decorated/doped structures can be controlled by varying the relative ratio of deposition lengths/rates of two or more sources. We have demonstrated that when doped with a small amount of catalyst (like Ti or V), well-aligned nanorod array, not the nanoblades, formed. This may be due to the pinning of catalyst atoms for Mg adatoms diffusion.

Figures 2a-b and e-f show the top view and cross-sectional SEM images of the 4.6 at% V-decorated Mg nanoblades and V-doped Mg nanorods deposited at an incident angle of 70°, respectively. From the composition depth profiles of both nanostructures by EDX mapping their cross-sections (Figures 2c and g), it is clear that both Mg and V distribute almost uniformly throughout the entire nanostructure height. In order to visualize the difference of fine structure of V on/in Mg matrix in both nanostructures, XRD, TEM and SAED were characterized. The results show that, for the V-decorated Mg nanoblades, the V exists in the form of randomly oriented crystals of ~5 nm diameter, in terms of the TEM (inset in Figure 2d), XRD (Figure 3a), and SAED (Figure 2d); while for the V-doped Mg nanorods, the V could exist in the Mg matrix in the form of atoms and/or very small clusters due to its undetectability by SAED (Figure 2h) and XRD (Figure 3b). Specifically, for the V-decorated Mg, the ED pattern (Figure 2d) is composed of the diffraction rings of V crystals and the diffraction spots of single crystal Mg; while for the

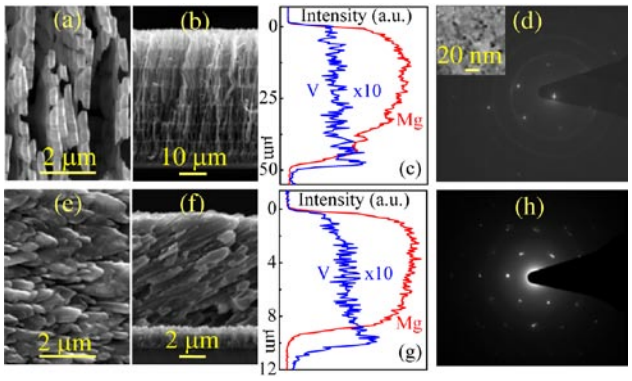

FIGURE 2. Top view and cross-section view SEM images of the as-deposited 4.6 at% V-decorated (a, b) and -doped Mg (e, f) nanostructures at 70°; (c, g) the composition depth profiles by EDX of the cross-sections b, f); the SAED patterns of V-decorated Mg nanoblade (d) and V-doped Mg nanorod (h); the inset in (d) is the TEM image, showing Mg matrix decorated with V particles of ~5 nm diameter.

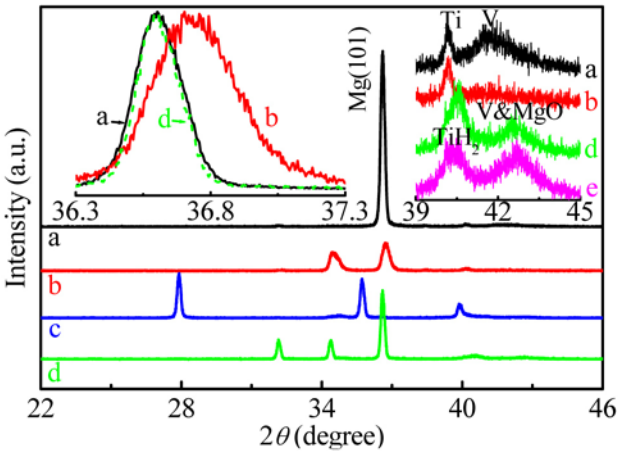

FIGURE 3. Typical XRD patterns of both nanostructures before and after H-cycling: (a) the as-deposited V-decorated Mg nanoblades; (b) the as-deposited V-doped Mg nanorods; (c) the hydrogenated and (d) the dehydrogenated V-doped Mg nanorods; (e) the hydrogenated V-decorated Mg nanoblades. The zoom-in patterns in the top left inset show the Mg peak shift to a higher angle due to the V-doping and its shift back after H-cycling. The zoom-in patterns in the top right inset show the difference and similarity in the as-deposited and H-cycled two nanostructures.

V-doped Mg, only the diffraction spots of single crystal Mg appear in the ED pattern (Figure 2h). Their XRD results are shown in Figure 3. For both the as-deposited samples, the dominate XRD peaks are from hexagonal Mg, as shown in Figure 3a for the V-decorated Mg and Figure 3b for the V-doped Mg. However, there are three differences between them. First, the former has an extremely strong Mg (101) peak at $2\theta \approx 36.60°$ compared to the latter. Second, by zooming in the Mg (101) peak shown in the top left inset, this Mg peak shifts toward a high diffraction angle $2\theta \approx 36.75°$ in the V-doped Mg sample, implying that the V is indeed doped into the Mg matrix and thus produces a stress [3]. Third, by zooming in the patterns ranging from 39° to 45° shown in the top right inset, a broad and weak V signal around 42° is visible in the V-decorated Mg, corresponding to nanocrystalline V grains of ~5 nm in diameter by Scherrer's formula [7], but not in the V-doped Mg, indicating that the V element in the doped sample is doped in the Mg in the forms of atoms or very small clusters. These results show that using this unique two-source GLAD system, one can tailor and design sophisticated metal and alloy nanostructures with/without nanocatalysts for hydrogen storage applications.

The Design of Novel Ti Barrier to Prevent Mg_2Si Formation in the H-Cycling of Mg/Si

Our experiments have revealed that Mg_2Si alloy can form even at a temperature as low as T = 200°C when Mg is deposited directly on Si substrate. This reaction strongly affects the hydrogen storage reversibility and cycling performance, and prohibits a good understanding of intrinsic H-nanostructure interactions. To prevent Mg/Si alloying, we have designed and fabricated a unique Ti nanostructure diffusion barrier using the shadowing effect of the GLAD technique (Figure 4).

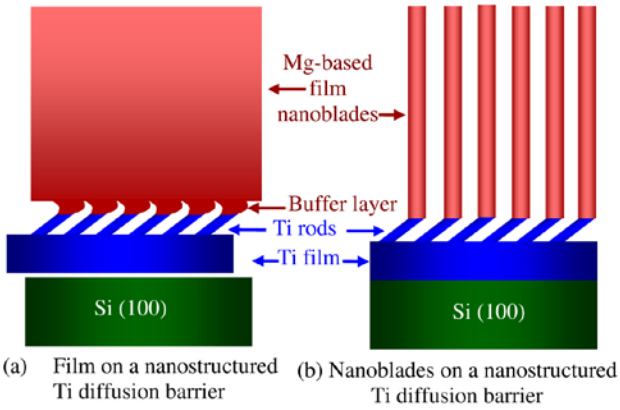

FIGURE 4. Design for a diffusion barrier layer composed of a Ti film and a Ti nanorod array on Si substrate, and then growing a layer of either Mg-based film (a) or nanoblade array (b) on top of the Ti nanorods.

We first deposited a 1 μm Ti film on the Si substrate, then a 500 nm Ti nanorods on the Ti film, followed by depositing Mg thin films or nanostructures directly on the Ti nanorod arrays, so that the Mg structures are lifted from the substrate. In fact, the V-decorated and doped Mg nanostructures in Figure 2 were grown on the unique Ti barriers, which can be seen in the cross-sectional SEM images (Figure 2) and detected by XRD. Our H-cycling experiments demonstrate that this Ti structure can endure over 15 hydrogenation-dehydrogenation cycles for the hydrogen storage kinetic and thermodynamic study of film-based Mg nanostructures with/without nanocatalyst. V-decorated

and -doped Mg nanostructures in Figure 2 were grown on the Si substrates with layers of 500 nm Ti nanorods at 70° and 1 µm Ti film at 10° in between the Mg samples and Si substrates. The Ti barrier can be seen in the cross-sectional SEM images (Figure 2) and detected by XRD (the inserted patterns of Figure 3).

MgH_2 Nanowire Formation during the Hydrogenation of Ti-Doped Mg Film

Once the Mg_2Si alloy formation is eliminated for hydrogenation of Mg thin film by the special barrier layer, new hydrogenation phenomenon has been observed during the hydrogenation of pure and Ti-doped Mg thin film. When 2 at% Ti-doped Mg film (with Ti barrier layers) has been hydrogenated at temperatures T <300°C for approximately 150 h, tetragonal single crystal MgH_2 nanowires are formed on the surface of Ti-doped Mg film, as shown in Figure 5. Figure 5a exhibits sections of some long and thin nanowires. These nanowires are very smooth and uniform. And some nanowires are short and thick, as shown in Figure 5b. This particular nanowire grew out from the sample surface, and the protruded end became distorted. The nanowires have diameters in the range of 200–700 nm, and most of them are below 400 nm. Also, for the wires thinner than 400 nm, the nanowires can grow very long, with lengths up to 500 µm or longer, while for those thicker than 400 nm, the nanowires are very short, only tens of microns or even shorter. The crystal structure and composition of the nanowires are confirmed to be tetragonal single crystal MgH_2 by XRD, Raman spectroscopy, EDX and TEM. Figure 5c shows a typical Raman spectrum obtained from the hanged nanowires in the inserted image. There are three Raman peaks centered at 312, 954, and 1,279 cm^{-1}, respectively. The 312 cm^{-1} and 954 cm^{-1} peaks are strong and sharp, while the 1,279 cm^{-1} peak is relatively weak and broad with a shoulder at its low wave-number side. The three peaks correspond to the characteristic vibration modes, B_{1g}, E_g, and A_{1g}, of tetragonal MgH_2. Our results show that the hydrogenation time and temperature are the two main factors for the nanowire formation.

The Hydrogenation and Dehydrogenation of V-Decorated and Doped Mg Nanostructures

The V-decorated and -doped Mg nanostructures were respectively installed in a PCT Sievert's-type apparatus (Hy-Energy, PCTPro-2000) for H-absorption (under 10-bar H-pressure) and desorption (under vacuum) cycling measurements. Their H-sorption kinetics were measured at various temperatures below 300°C, and the sorption rate constants k at different temperature were calculated and are plotted with respect to inverse temperature 1/T in Figures 6e and f, for the hydrogen absorption and desorption processes. From

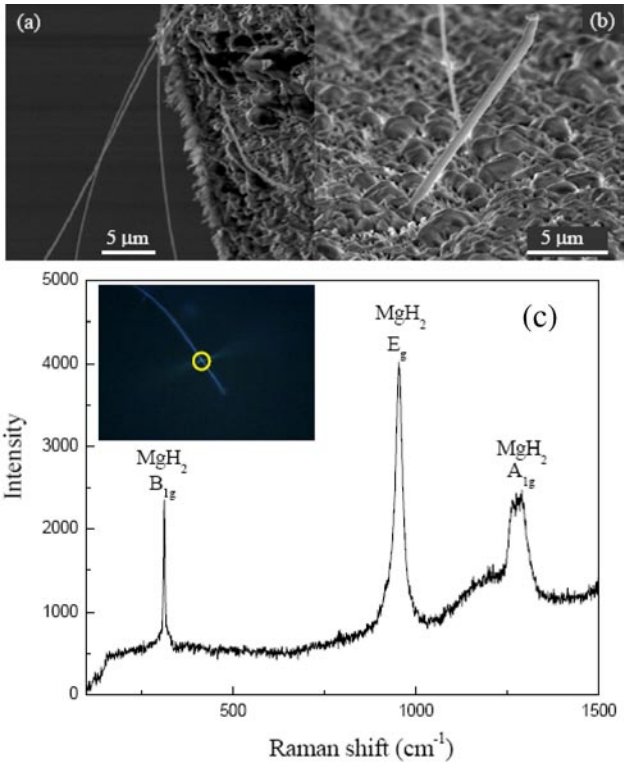

FIGURE 5. Typical top view SEM images of the hydrogenated 2 at% Ti doped Mg film sample showing (a) nanowires and (b) one whole nanowire formed on the sample surface. (c) Raman spectra obtained from individual nanowires shown by an inserted image.

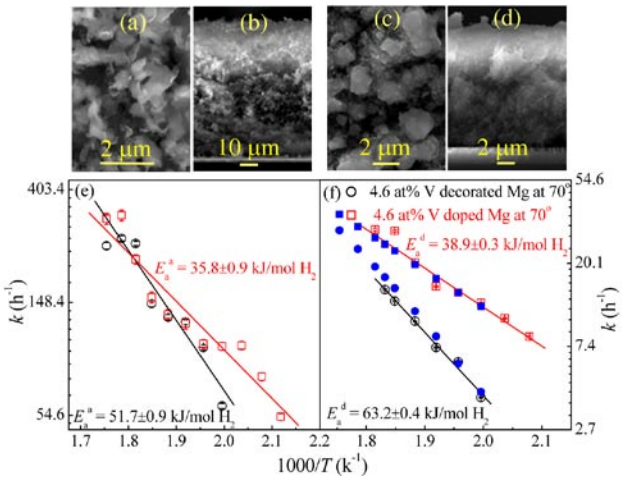

FIGURE 6. Top view and cross-section view SEM images of V-decorated (a, b) and -doped (e, f) Mg nanostructures at 70° after hydrogen cycling; Arrhenius plots of (e) H-absorption and (f) H-desorption rate constant *k* versus reciprocal temperature 1/*T* for both the 4.6 at% V-decorated and -doped Mg nanostructures. The calculated H-desorption *k* values, based on our proposed phenomenological model, are displayed in (f) by the solid circles and solid squares.

the Arrhenius plots in Figures 6e and f, we obtain that the activation energy of the 4.6 at% V-decorated Mg

sample is $E_a^a = 51.7 \pm 0.9$ kJ/mol H_2 for absorption process and $E_a^d = 63.2 \pm 0.4$ kJ/mol H_2 for desorption process, and the activation energy of the 4.6 at% V-doped Mg sample is $E_a^a = 35.8 \pm 0.9$ kJ/mol H_2 and $E_a^d = 38.9 \pm 0.3$ kJ/mol H_2. On one hand, these activation energies are much lower than the reported desorption energy of 141 kJ/mol H_2 for MgH_2 film and 156 kJ/mol H_2 for MgH_2 powder, indicating the catalytic effect of the incorporated V catalyst; on the other hand, the hydrogen sorption is faster for the V-doped Mg than the V-decorated Mg sample, and also the former has lower absorption and desorption activation energies than the latter, even though the V-decorated Mg (with a void ratio of ~668%) is more porous than the V-doped Mg structures (with a void ratio of only ~34%). After multiple cycles of hydrogen absorption/desorption, a significant morphology change occurs to both samples and they both present a very similar appearance: the original blade or rod structure is totally distorted to form aggregates of sphere-like particles, as shown by the SEM images in Figures 6a-b for the hydrogenated V-decorated Mg and Figures 6c-d for the hydrogenated V-doped Mg.

Figure 7 shows the obtained Arrhenius plots for the V-doped Mg nanostructures deposited at incident angles of 10°, 50°, and 70°. For the three nanostructures, the void ratio is estimated to ~4% of 10°, 14% of 50°, and 34% of 70° samples, respectively. From Figure 7, one can see that the hydrogen sorption becomes faster and faster with increasing the deposition angle or the porosity; the H-absorption activation energy decreases from Eaa = 51.4 ± 1.5 kJ/mol H_2 of the 10° sample, $E_a^a = 47.0 \pm 1.4$ kJ/mol H_2 of the 50° sample, to $E_a^a = 35.8 \pm 0.9$ kJ/mol H_2 of the 70° sample (Figure 7a); the hydrogen desorption activation energy decreases from $E_a^d = 69.4 \pm 0.6$ kJ/mol H_2 of the 10° sample, $E_a^d = 64.8 \pm 0.4$ kJ/mol H_2 of the 50° sample, to $E_a^d = 38.9 \pm 0.3$ kJ/mol H_2 of the 70° sample (Figure 7b). The improved hydrogen sorption performance could be caused by the smaller particles/grains with increasing the deposition angle.

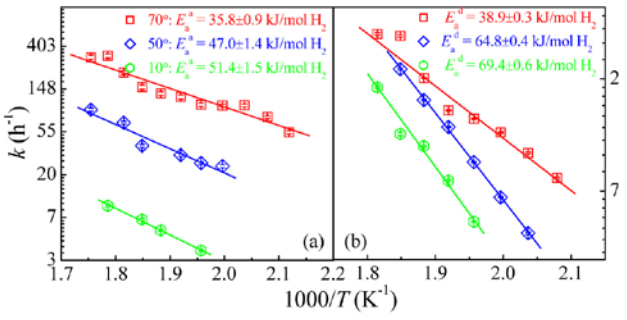

FIGURE 7. Arrhenius plots of (a) H-absorption and (b) H-desorption rate constant k versus reciprocal temperature 1/T for the 4.6 at% V-doped Mg nanostructures at 10°, 50°, and 70°.

5. FRES and RBS Results

FRES (forward recoiled spectrometry) measurements on metal hydride films have been carried out using the ion beam facility at UPenn (with Prof. Howard Wang). In FRES, a collimated 3.0 MeV He^{2+} beam incident on samples at 75° from the surface normal, recoiled H atoms were detected at the specular reflection direction, while the forward scattered He ions were stopped using a 12 μm thick aluminum foil. Figures 8a and b show FRES spectra of 4 μm pure Mg films and nanoblades after hydrogenation at various temperatures, respectively. The H uptake in Mg films is rather minimal at 300°C and below, whereas significant absorption of H in nanoblades occurs at a temperature as low as 200°C, suggesting lower activation barrier due to the large surface area. Figure 8(c) reveals slight H enrichment near film surfaces at low-T, possibly due to the water adsorption. The integrated total H uptake for two series is shown in Figure 8(d). It is apparent that activation of H absorption occurs at a lower T in Mg nanoblades, although the H saturation in nanoblades is lower.

6. Neutron Scattering Results

PGAA (prompt gamma-ray activation analysis) measurements have been carried out on V-doped and decorated Mg nanoblades in NIST by Prof. Howard Wang. A typical PGAA spectrum is shown in Figure 9, where characteristic activation peaks are used to identify the absolute amount of H, Mg and V in those samples. Careful analysis shows chemical stoichiometry of Mg:H:V = (1.00 ± 6.13%) : (1.72 ± 1.04%),: (0.0428 ± 1.48%) in the V-decorated sample and Mg:H:V = (1.00 ± 5.15%) : (2.00 ± 1.01%) : (0.0515 ± 1.29%) in the V-doped sample, respectively. Note the high accuracy

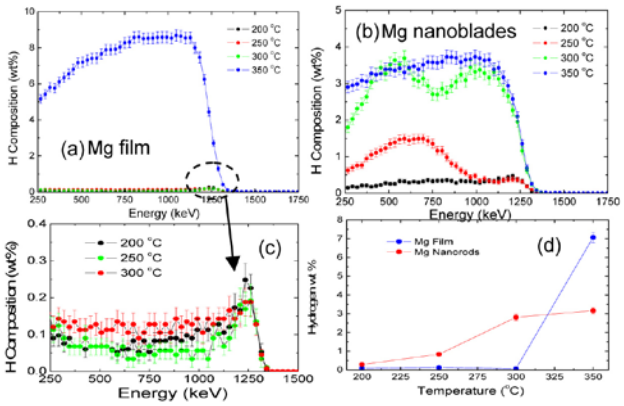

FIGURE 8. FRES measurements of hydrogen profiles of (a) Mg films and (b) Mg nanoblades after hydriding at various T. (c) The surfaces enrichment in films of low-T treatment. (d) Total H uptake for both films and nanoblades.

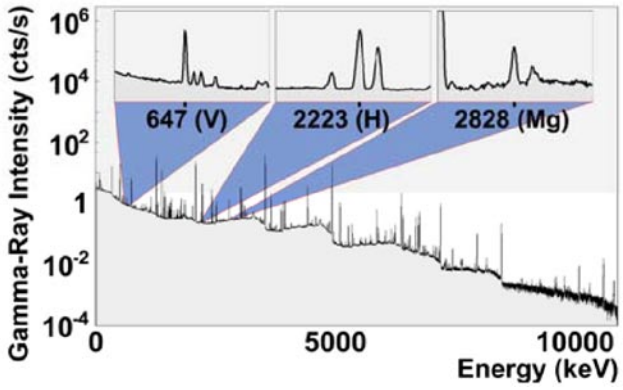

FIGURE 9. The PGAA spectrum of V-doped MgHx nanoblades. Insets show the characteristic γ-ray emissions for quantifying each element.

of absolute H quantification using PGAA. Within the experimental error, the theoretical limit of H absorption was reached in V-doped Mg nanoblades at a rather mild hydrogenation condition. Small angle neutron scattering (SANS) has also been used to measure the samples. The dominant characteristics are the Q^{-3} power law scaling in both samples, indicating 3D "cardhouse" packing, consistent with nanoblade structure shown in Figure 2.

7. In Situ Temperature-Dependent Raman Spectroscopy Measurements

Hydrogenated Mg nanostructures were investigated using temperature-dependent Raman spectroscopy. The Mg film substrates were fabricated by UGA using OAD at an incident vapor flux of 9.9°. The most prominent peak at 951 cm^{-1} becomes increasingly broadened as the temperature reaches 150ºC and above, but is still present at 180ºC. The center peak position did not shift in a noticeable manner but the peak clearly became broader as the temperature was increased. When the temperature is returned to room temperature, the peak recovers, indicating no thermal degradation of the sample. The lack of peak shifting indicates that even at these high temperatures, the lattice is not being distorted by expansion or anharmonic effects. The broadening of the band is understandable since higher temperature shortens the lifetimes of the excited vibrational or phonon states, which leads to spectral broadening. In conclusion, temperature-dependent Raman characterization helped to provide a more fundamental look into the effect of temperature on the hydrogen-Mg interaction for this sample.

Using the temperature and pressure controlled in situ Raman chamber, layered magnesium films (Mg rods/Ti barrier layer/Si wafer substrate) fabricated by UGA were investigated to see if the hydrogenation of the sample could be monitored with Raman spectroscopy. Unfortunately, higher temperatures are needed to induce an observable amount of MgH_2 formation through Raman spectroscopy and our current chamber has limitations of both temperature (250°C) and pressure (100 psi) which inhibit our ability to monitor the hydrogenation and the dehydrogenation of the hydrogenated films. Extended periods of times were used at the chamber's maximum temperature and pressure but no hydrogen sorption was observed. Future adjustments will be made to the chamber to ensure a wider range of temperatures which could aid the fundamental understanding of such materials and thus help to eventually lower those dehydrogenation temperatures.

Publications since the Beginning of the Project

1. W.M. Hlaing Oo, M.D. McCluskey, A.D. Lalonde and M.G. Norton, "Infrared spectroscopy of ZnO nanoparticles containing CO_2 impurities," *Appl. Phys. Lett.* **2005**, 86, 073111.

2. W.M. Hlaing Oo, M.D. McCluskey, J. Huso and L. Bergman, "Infrared and Raman spectroscopy of ZnO nanoparticles annealed in hydrogen," *Journal of Applied Physics* **2007**, 102(4), 043529.

3. Y.-P. He, J.-S. Wu and Y.-P Zhao, "Designing Catalytic Nanomotors by Dynamic Shadowing Growth," *Nano Lett.* **2007**, 7(5), 1369-1375.

4. Y.-P. He, J.-X. Fu, Y. Zhang, Y.-P. Zhao, L.-J. Zhang, A.-L Xia and J.-W. Cai, "Multilayered Si/Ni Nanosprings and Their Magnetic Properties," *Small* **2007**, 3(1), 153-160.

5. Rebecca Newhouse, Leo Seballos, J. Z. Zhang, Eric Majzoub, and Ewa Ronnebro, "Temperature dependent Raman scattering study of $LiAlH_4$ and Li_3AlH_6," *SPIE Proc.* **2007**, 6650, 0N1-0N6.

6. Y.-P. He, Y.-P. Zhao and J.-S. Wu, "The effect of Ti doping on the growth of Mg nanostructures by oblique angle codeposition," *Appl. Phys. Lett.* **2008**, 92(6), 063107.

7. Y.-P. He, Z.-Y. Zhang, C. Hoffmann and Y.-P. Zhao, "Embedding Ag Nanoparticles into MgF_2 Nanorod Arrays," *Advanced Functional Materials* **2008**, 18(11), 1676–1684.

8. R. Blackwell and Y.-P. Zhao, "Metal nanoparticle embedded porous thin film prepared by oblique angle co-evaporation," *J. Vac. Sci. Technol. B* **2008**, 26, 1344-1349.

9. Y.-P. He, Y.-J. Liu and Y.-P. Zhao, "The formation of MgH2 nanowires during the hydrogenation of Ti-doped Mg film," *Nanotechnology* **2008**, 19(46), 465602.

10. Y.-P. He, Y.-P. Zhao, L.-W. Huang, H. Wang and R.J. Composto, "Hydrogenation of Mg film and Mg nanoblade array on Ti coated Si substrates," *Appl. Phys. Lett.* **2008**, 93(16), 163114.

11. J.-X. Fu, Y.-P. He and Y.-P. Zhao, "Fabrication of Heteronanorod Structures Using Dynamic Shadowing Growth," *IEEE Sensors* **2008**, 8(6), 989-997.

12. W.M. Hlaing Oo, M.D. McCluskey, Y.-P. He and Y.-P. Zhao, "Strong Fano resonance of oxygen-hydrogen bonds

on oblique angle deposited Mg nanoblades," *Appl. Phys. Lett.* **2008**, 92(18), 183112.

13. Y.-P. He and Y.-P. Zhao, "Improved hydrogen storage properties of V decorated Mg nanoblade array," Physical *Chemistry Chemical Physics*, **2009**, 11(2), 255-258.

14. Y.-P. He and Y.-P. Zhao, "Hydrogen storage and cycling properties of vanadium decorated Mg nanoblade array on Ti coated Si substrate," *Nanotechnology* (in press).

15. Y.-P. He and Y.-P. Zhao, "The role of Mg_2Si formation in the hydrogenation of Mg film and Mg nanoblade array on Si substrates," *Journal of Alloys and Compounds* (in press).

16. Leo Seballos, Jin Z. Zhang, Ewa Ronnebro, Julie L. Herberg, and E.H. Majzoub, "Metastability and crystal structure of the bialkali complex metal borohydride $NaK(BH_4)_2$," Journal of Alloys and Compounds, (in press).

17. Y.-P. He and Y.-P. Zhao, "The morphology of Mg nanostructures tailored by glancing angle deposition on patterned substrate," in preparation.

18. Y.-P. He and Y.-P. Zhao, "The role of V-catalyst distribution in the hydrogen storage performance of Mg nanostructures," in preparation.

19. Rebecca Newhouse, Jin Z. Zhnag, Rönnebro, E, C. Jensen, G. Severa, "Direct Synthesis and characterization of Magnesium Borohydride", in preparation.

Personnel Associated with the Research

- At UGA

Dr. Yuping He	Postdoc	100%
Chris Hoffman	Undergraduate Student	
Robert Blackwell	Undergraduate Student	
Dr. Yiping Zhao (PI)		

- At UCSC

Leo Sabellos	PhD Student	80%
Rebecca Newhouse	PhD Student	80%
Nicole Richards	PhD Student	20%
Dr. Jin Z. Zhang (co-PI)		

- At WSU

Win Maw Hlaing Oo	PhD Student	100%
Dr. Matthew D. McCluskey (co-PI)		